The American Society of Mechanical Engineers

Reprinted From
HTD—Vol. 214, Bifurcation Phenomena and Chaos in Thermal Convection
Editors: H. H. Bau, L. A. Bertram, and S. A. Korpela
Book No. G00699—1992

CHAOS AND SYMBOL SEQUENCES IN SYSTEMS WITH A PERIODICALLY-DISAPPEARING FIGURE-EIGHT SEPARATRIX

Jacqueline Bridge and Richard Rand
Department of Theoretical and Applied Mechanics
Cornell University
Ithaca, New York

ABSTRACT

This work concerns the dynamics of slowly varying Hamiltonian systems which possess a figure–eight separatrix which periodically disappears. Such situations occur in familiar mechanical systems such as a dynamically buckled beam or a rotating plane pendulum.

The dynamics of such a system may be characterized by noting the position of a motion once per forcing cycle, as being in the right loop (R), the left loop (L) or outside the separatrix loops (O), thereby generating a symbol sequence of R's, L's and O's. We show that the resulting RLO sequence exhibits sensitive dependence on initial conditions, a criterion for chaos.

By investigating a variety of examples, we identify the complex dynamical behavior in this class of systems as coming from several sources: effects of stretching along the unstable manifold of the saddle, quasiperiodic rotation, separatrix crossing and Hamiltonian chaos.

INTRODUCTION

This work is concerned with dynamical systems which are slowly varying, i.e., which involve two time scales: one time scale describes the "instantaneous" dynamics, while the other time scale ("slow time") describes the slow evolution of the instantaneous dynamics. In particular, we are interested in systems which are slowly and periodically forced to change the qualitative nature of their instantaneous dynamics. We consider a class of single degree of freedom systems in which the origin (in phase space) is an equilibrium point whose stability periodically changes. We omit damping from our considerations, and thus the origin periodically changes from an instantaneous center to an instantaneous saddle. When the origin is a saddle, we further assume that the phase portrait includes an instantaneous separatrix in the form of a figure–eight (a double homoclinic loop), i.e., that two additional instantaneous centers exist, see Fig.1.

A system which exhibits this kind of behavior is the nonlinear Mathieu equation,

$$x'' - x\cos\epsilon t + x^3 = 0 \tag{1}$$

in which we assume that $\epsilon<<1$ (slow forcing). The instantaneous separatrix in eq.(1) slowly grows and then slowly shrinks during the half of the forcing cycle in which it exists. Although a trajectory cannot cross a real separatrix, an instantaneous separatrix represents no such barrier, and separatrix crossing plays a significant role in the dynamics of eq.(1).

In order to evaluate the process of slow evolution in eq.(1), we will also consider a related system which does not involve slow evolution: the nonlinear Meissner equation,

$$x'' - x\,\mathrm{sgn}(\cos\epsilon t) + x^3 = 0 \tag{2}$$

In contrast to eq.(1), in which the dynamics are truly slowly varying, in eq.(2) there is a sudden jump between the two kinds of phase portraits. The separatrix in eq.(2) remains unchanged for half the forcing cycle, at the end of which it suddenly disappears.

As an example of a physical system which exhibits these features, consider an elastic column in which the axial force is slowly and periodically varied so that sometimes it is larger than the Euler bucking load, and sometimes smaller. During those times when the axial force is larger than the buckling load, the column will tend to move away from its undeformed state (the origin in the foregoing discussion, now unstable) and will tend to oscillate about one of the two buckled states (corresponding to the two additional instantaneous centers), or possibly in a larger amplitude motion (corresponding to motions in the phase plane which circulate around the outside of the separatrix).

A simple model of an elastic column is shown in Fig.2, and consists of two weightless rods of length L attached to a mass m. The rods are pinned at their ends and their motion is restrained by a linear torsion spring with spring constant k. The structure is loaded by a pair of compressive forces $P(\tau)$, and the displacement of the mass is u. The equation of motion for this system has been derived by Stoker ([16], p.54):

$$m\frac{d^2u}{d\tau^2} - 2\frac{P\,u - k\,\arcsin(u/L)}{\sqrt{L^2 - u^2}} = 0 \tag{3}$$

The Euler buckling load for this structure is $P = k/L$. We set

$$P = \frac{k}{L} + A\cos\omega\tau \tag{4}$$

We normalize by changing variables from $u(\tau)$ to $x(t)$, where

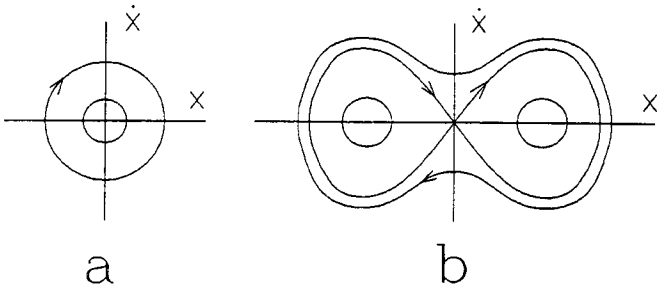

Fig.1. Instantaneous phase portraits for a dynamical system which periodically changes from a) rotation phase to b) separatrix phase.

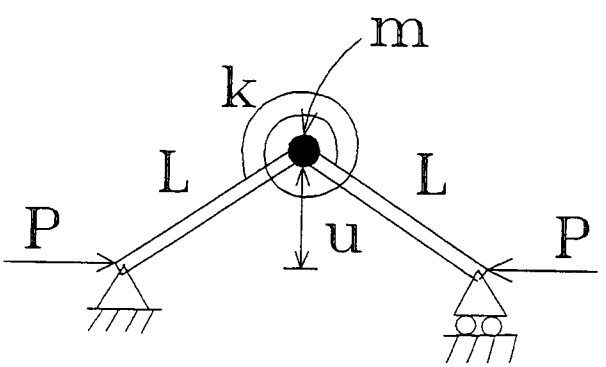

Fig.2. A simple model of an elastic column.

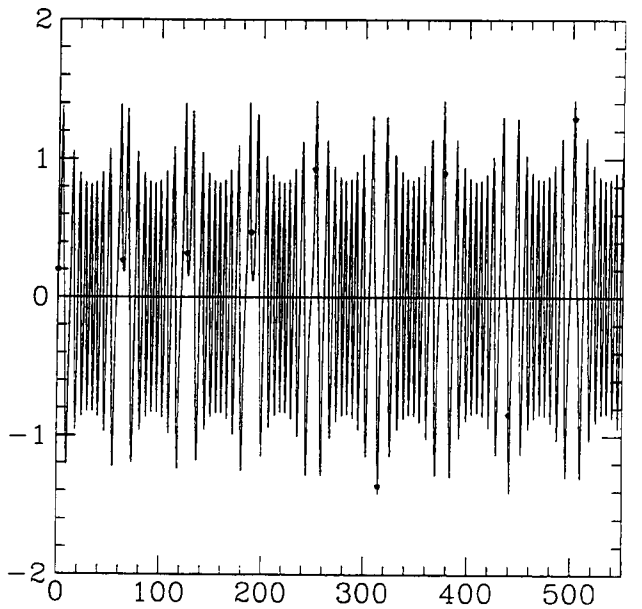

Fig.3. Numerical integration of the nonlinear Mathieu eq.(1) with $\epsilon = .1$ for the initial condition $x(0) = .20$, $x'(0) = 0$. The horizontal axis is time t and the vertical axis is x. Dotted points represent x at the stroboscopic times $t = 0, 2\pi/\epsilon, 4\pi/\epsilon, \ldots$. Each such point corresponds to a symbol: R if the motion lies inside the right separatrix loop, L for the left loop, and O outside of both loops. The indicated RLO sequence is RRR ROO OOO.

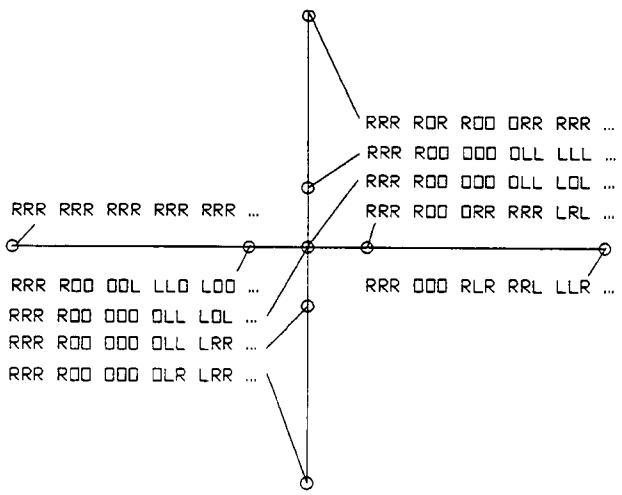

Fig.4. RLO sequences for two rosettes of four points each, centered about $x = 0.2$, $x' = 0$. The radius of the outer rosette is .01, and of the inner rosette is .0001. Results were obtained by numerically integrating eq.(1) with $\epsilon = 0.1$.

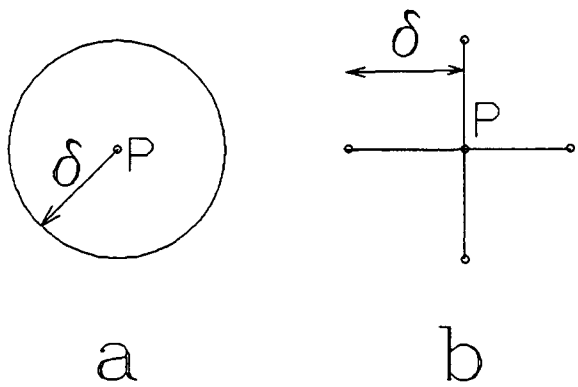

Fig.5. a) The δ–insensitivity of a point P is defined to be the minimum RLO propinquity of all initial conditions located on a circle of radius δ with center at P.

b) An approximate value for the δ–insensitivity of P may be obtained as the minimum of the RLO propinquities of a rosette of four initial conditions.

(5) $u = [3\,\epsilon\,\beta]^{1/2}\,x, \quad \tau = \epsilon^{-1/2}\,t, \quad \omega = \epsilon^{3/2}, \quad \beta = mL^4/k$

and where $\epsilon = \frac{2A}{mL}$ is assumed to be small. Expanding for small ϵ, we obtain eq.(1) to leading in order in ϵ.

In addition, eq.(1) has been shown to govern the dynamics of a plane pendulum, the plane of which is forced to rotate about a vertical axis [7].

SYMBOL SEQUENCES

We shall see that the two systems (1) and (2) exhibit similar dynamical behavior. In particular, they both exhibit chaos. We shall identify the chaotic behavior by using a symbol sequence, defined as follows: We examine the position of a motion once per forcing cycle, at the stroboscopic times $t = 0, 2\pi/\epsilon, 4\pi/\epsilon, \ldots$, and note whether the motion lies in the right loop (R), the left loop (L), or outside of both loops (O). For a given initial condition, this results in a sequence of symbols, each of which is either an R,L or O. See Fig.3. Our investigations show that the resulting RLO sequence is sensitive to a small change in initial conditions, a criterion for chaos.

By way of illustration, consider the dynamics of eq.(1) with $\epsilon = 0.1$. For a given initial condition we can find, by using numerical integration, an associated RLO sequence. For example, choosing the point (.2,0) arbitrarily,

x(0)= .20	x′(0)= 0	RRR ROO OOO OLL LOL...

where we have spaced the symbols in groups of three for ease in reading them. Now consider a rosette of four initial conditions, each of which is a distance of 0.01 from (.2,0), each respectively displaced from (.2,0) in the one of the directions of the coordinate axes:

x(0)= .19	x′(0)= 0	RRR RRR RRR RRR RRR...
x(0)= .21	x′(0)= 0	RRR OOO RLR RRL LLR...
x(0)= .20	x′(0)= −.01	RRR ROO OOO OLR LRR...
x(0)= .20	x′(0)= .01	RRR ROR ROO ORR RRR...

See Fig.4. Note that each of these initial conditions ceases to have the same RLO sequence as (.2,0) after a certain number of forcing periods. We have found it convenient to define the RLO propinquity between two initial conditions as the number of leading symbols their RLO sequences have in common. Thus each of the four initial conditions has a RLO propinquity from (.2,0) of 4,3,11 and 5, respectively.

Consider now a similar rosette of four initial conditions, but this time let their distance from (.2,0) be .0001:

x(0)=.1999	x′(0)= 0	RRR ROO OOL LLO LOO...
x(0)=.2001	x′(0)= 0	RRR ROO ORR RRR LRL...
x(0)=.2000	x′(0)=−.0001	RRR ROO OOO OLL LRR...
x(0)=.2000	x′(0)=.0001	RRR ROO OOO OLL LLL...

Each of these initial conditions has a RLO propinquity from (.2,0) of 8,7,13 and 13, respectively.

Comparing the above results, we observe that as the distance between two initial conditions becomes smaller, the RLO propinquity between them generally becomes larger. Nevertheless no matter how close an initial condition is taken to (.2,0), after a sufficiently long time their RLO sequences will cease to be identical.

Having made the foregoing observations, we now will utilize the concept of RLO propinquity to produce a graphical description of the dynamics of eq.(1). Given an initial condition P, consider all neighboring initial conditions which lie on a circle of radius δ with center at P. We define the δ–insensitivity of P to be the minimum RLO propinquity of all initial conditions located on a circle of radius δ with center at P. An approximate value for the δ–insensitivity may be obtained by computing the RLO propinquities of a rosette of four initial conditions, as above. See Fig.5. For example, based on the above results, we approximate the .01–insensitivity of (.2,0) to be 3, and the .0001–insensitivity of (.2,0) to be 7. The intuitive notion that the RLO sequence shows sensitive dependence on initial conditions (SDIC) may now be stated quantitatively in terms of local values of δ–insensitivity, with small values of δ–insensitivity corresponding to greater SDIC.

Using these ideas together with numerical integration of eq.(1) for ϵ=0.3, we produced Fig.6, which displays both the .02– and .0075–insensitivities for a region of initial conditions. We see that the insensitivity is lowest near the separatrix itself, and that the region inside the separatrices and nearby the outside of the separatrices are filled with fine structure. Motions starting far outside the separatrix tend to have RLO sequences which begin with a large number of O's, and hence have high insensitivities.

In order to gain a better understanding of Fig.6, consider the case of two neighboring initial conditions which have RLO sequences with propinquity 1, e.g. RO ... and RR ... . After one forcing period, these points which were originally close to each other inside the same region (R here), find themselves on opposite sides of an instantaneous separatrix. Thus a straight line connecting the two initial conditions must have a point on it which, after one forcing period, is mapped into the instantaneous separatrix itself (by continuity). Conversely, let us start with the set of all points on the instantaneous separatrix at t=0 and run the system backwards for one forcing period, and let us denote by S_{-1} the resulting set of points. If we then run the system forward, initial conditions near S_{-1}, but on opposite sides of it, would end up with different RLO symbols after one forcing period, i.e., S_{-1} is the locus of points with RLO insensitivity 1. See Fig.7, where S_{-1} is displayed for eq.(1) with ϵ=0.3. In this Figure, the set S_{-1} is obtained by starting with 10000 initial conditions inside the right separatrix loop at t=0 and numerically integrating backwards in time for one forcing period, thus yielding S_{-1} as the boundary of the darkened region. This scheme is chosen instead of the more direct approach of starting with a large number of initial conditions on the separatrix itself because of the great extent of stretching along the unstable manifold of the saddle, i.e., some very tiny intervals of the t=0 separatrix get tremendously elongated, leaving gaps in the resulting representation of S_{-1}. (The same scheme is used in Figs.8, 10 and 11, except that 30000 initial conditions are used in the latter two Figures.)

In a similar fashion, if we let S_{-n} represent those initial conditions which are mapped into the instantaneous separatrix after n forcing periods, then S_{-n} will be the locus of points with RLO insensitivity n. See Fig.8, where S_{-2} is displayed for eq.(1) with ϵ=0.3.

Thus the fine structure exhibited by Fig.6 may be related to the sets S_{-n}. At a point where S_{-n} and S_{-m} intersect, the RLO insensitivity is the smaller of m and n, although such points of intersection represent a set of measure zero. The shape of the sets S_{-n} are influenced by the contraction near the saddle along its stable manifold and the expansion along its unstable manifold. Note that eqs.(1) and (2) are both reversible, so that the sets S_{-n} and S_n have the same shape, except that one is a mirror image of the other.

COMPARISON OF NONLINEAR MATHIEU AND MEISSNER EQUATIONS

We have seen that the RLO dynamics of eq.(1) can be described by RLO insensitivity plots and backwards iterates of the instantaneous separatrix, Figs.6–8. In order to compare the dynamics of eq.(1) with those of eq.(2), we present in Figs.9–11

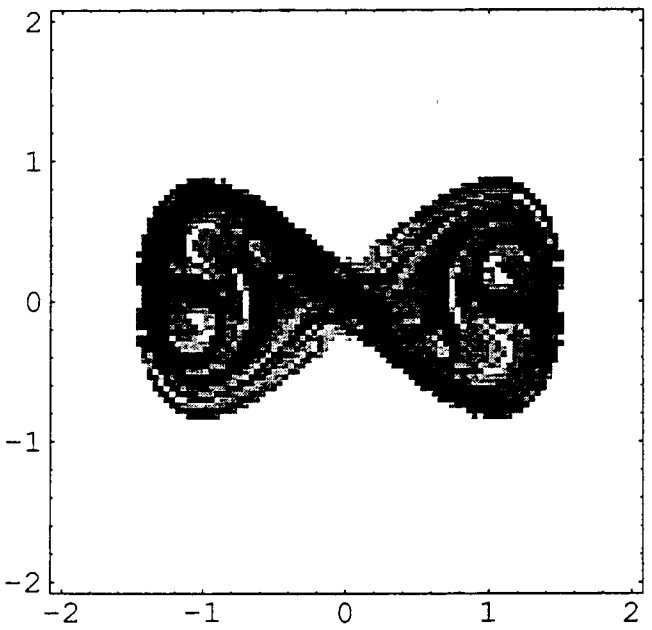

Fig.6a. RLO .02–insensitivity plot for the nonlinear Mathieu eq.(1) with $\epsilon = 0.3$. A region of the x–x′ plane is displayed. Insensitivity is color–coded with six shades of grey. White corresponds to an insensitivity of 5 or greater, and black to an insensitivity of 0. Results obtained by numerical integration of eq.(1).

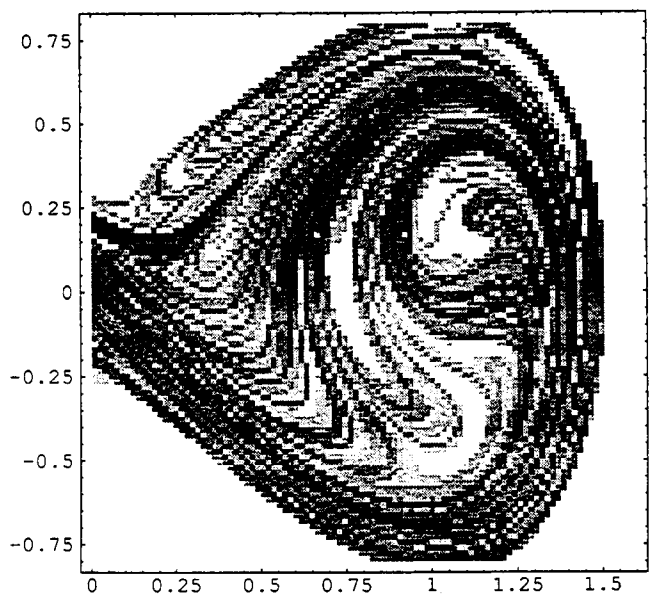

Fig.6b. RLO .0075–insensitivity plot for the nonlinear Mathieu eq.(1) with $\epsilon = 0.3$. A region of the x–x′ plane is displayed. Insensitivity is color–coded with six shades of grey. White corresponds to an insensitivity of 5 or greater, and black to an insensitivity of 0. Results obtained by numerical integration of eq.(1).

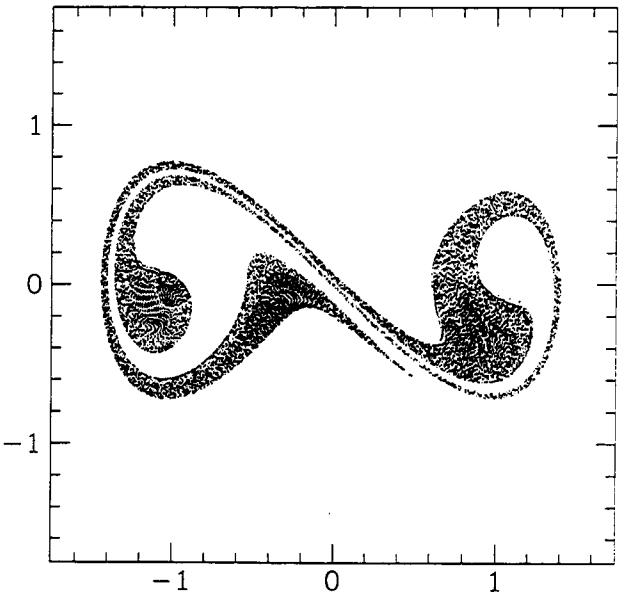

Fig.7. The set S_{-1} for the nonlinear Mathieu eq.(1) with $\epsilon = 0.3$. Displayed is a map, backwards in time for one forcing period, of initial conditions in the x–x′ plane located inside the right separatrix loop . Thus S_{-1} is the boundary of the darkened region. Since only the right loop is mapped, we see only half of the set S_{-1}. The missing part is a reflection in the origin of the part shown.

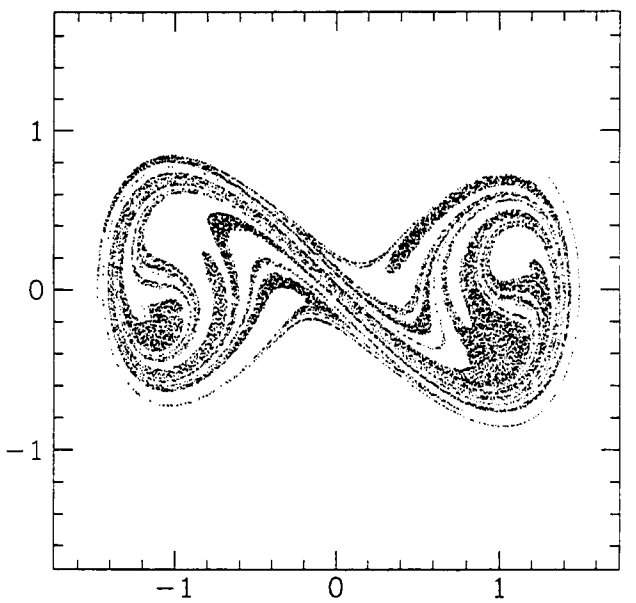

Fig.8. The set S_{-2} for the nonlinear Mathieu eq.(1) with $\epsilon = 0.3$. Displayed is a map, backwards in time for two forcing periods, of initial conditions in the x–x′ plane located inside the right separatrix loop . Thus S_{-2} is the boundary of the darkened region. Since only the right loop is mapped, we see only half of the set S_{-2}. The missing part is a reflection in the origin of the part shown.

comparable plots for eq.(2) with ϵ=0.3 to those of Figs.6–8 for eq.(1) with ϵ=0.3. Unlike Figs.6–8, which were obtained by numerical integration of eq.(1), Figs.9–11 are based on an exact solution to eq.(2) in terms of elliptic functions (see [4] for details). This permits the associated computations to be done more efficiently.

Examination of Figs.6 and 9 shows that the RLO insensitivity plots for both the nonlinear Mathieu eq.(1) and the nonlinear Meissner eq.(2) exhibit a great deal of fine structure and complexity. Comparison of Figs.7,8 with Figs.10,11 shows that the extent of S_{-1} and S_{-2} is greater in eq.(2) than in eq.(1), i.e., the "diffusion" of chaos outward from the immediate neighborhood of the separatrix is greater in eq.(2). This is due to the fact that in eq.(1) trajectories must cross the (instantaneous) separatrix to move outside of a separatrix loop, a gradual process which we shall look at later in this paper. In eq.(2), however, a motion can be inside a separatrix loop at the start of the half–cycle when then the separatrix suddenly disappears, and then be rotated to lie outside the separatrix loops when they reappear a half–cycle later.

SOURCES OF CHAOS

We have seen that the sensitive dependence on initial conditions [9] exhibited by the RLO sequence is a measure of the chaos in systems like eqs.(1) and (2). This chaos may be associated with the increase in perimeter of S_{-n} as n increases, due to the stretching of the flow along the unstable manifold of the saddle. Since S_{-n} is the locus of points with RLO insensitivity n, an increase in the perimeter of S_{-n} will cause the RLO sequences of a larger set of points to differ from those of their neighbors after n symbols.

An additional source of chaos in these systems is Hamiltonian chaos, which has been widely discussed in the literature [11] and is assumed to be familiar to the reader. The occurrence of Hamiltonian chaos in these systems is due to the absence of damping, and may be illustrated by showing a sample Poincare map for eq.(1), see Fig.12.

The rotation phase, in which the separatrix has disappeared, is another source which complicates the system dynamics. In order to isolate this effect, we may consider the linear Mathieu equation by omitting the x^3 term in eq.(1):

$$x'' - x\cos\epsilon t = 0 \tag{6}$$

An approximate solution to eq.(6) in the form of an asymptotic expansion using the WKB method and computer algebra (MACSYMA) has been obtained in [4]. It has been shown [4] that the zero solution of eq.(6) is stable for an infinite number of intervals on the ϵ axis. Note that eq.(6) governs the stability of the origin in the nonlinear Mathieu eq.(1). If ϵ is chosen so that the origin is stable, then the effect of the rotation phase in eq.(6) is to produce a quasiperiodic motion. The resulting symbol sequence reflects this quasiperiodicity. The same situation applies to the linear Meissner eq., i.e. eq.(2) without the x^3 term.

Although the rotation phase contributes to the complex behavior of eq.(1) by combining quasiperiodic rotations with the slow motion of the instantaneous separatrices, the rotation phase is not necessary for chaotic behavior. This may be demonstrated by modifying eq.(1) so that it has no rotation phase, and then using separatrix crossing theory to obtain approximate symbol sequences.

SEPARATRIX CROSSING THEORY

The work presented in this section is based on results obtained by Henrard [10], Cary et al. [5], Neishstadt [14], and others [1,2,3,6,8,13,15]. It is a perturbation off of the "frozen" motion around the separatrix, and it assumes that the motion remains in the vicinity of the separatrix for all time. In order to modify eq.(1) so that it has no rotation phase, we select the slowly varying periodic coefficient so that it remains negative for all t, varying between –1 and –2:

$$x'' + f(\epsilon t)\,x + x^3 = 0 \tag{7}$$

$$f(\epsilon t) = -\tfrac{1}{2}(3 + \cos 2\pi\epsilon t) \tag{8}$$

In order to use Henrard's results [10], we recast eq.(7) into Hamiltonian form:

$$H = \tfrac{1}{2}p^2 + \tfrac{1}{2}f(\epsilon t)\,q^2 + \tfrac{1}{4}q^4 \tag{9}$$

For the associated frozen system, $f(\epsilon t)$ is treated like a constant. In this case H remains constant in time and the integral curve through the origin corresponds to a separatrix. On this separatrix, H = 0 and we find

$$p = \pm\left[-f\,q^2 - \tfrac{1}{2}q^4\right]^{1/2} \tag{10}$$

From eq.(10), the area J inside one of the separatrix loops (i.e. the "action") is given by the following integral, which may be evaluated in closed form:

$$J = \int p\,dq = \tfrac{4}{3}(-f)^{3/2} \tag{11}$$

Henrard [10] derives an expression for the change in energy which a motion undergoes when it travels close to the separatrix in the slowly–varying (non–frozen) system. After passing completely around one of the separatrix loops, the change in energy ΔH is approximately:

$$\Delta H = -\frac{\partial J}{\partial t} \tag{12}$$

which becomes, from eqs.(11) and (8),

$$\Delta H = \sqrt{2}\pi\epsilon \sin 2\pi\epsilon t\,[3 + \cos 2\pi\epsilon t]^{1/2} \tag{13}$$

Using eq.(13) we can obtain the approximate change in energy level as the system moves from a point near the origin on one of the four coordinate axes to the next such point on its trajectory. See Fig.13 where the points U,R,D and L represent points of intersection of a trajectory with the coordinate axes. E.g., a point starting at U may travel around the outside of the right loop to D, or (less typically) it may cross the instantaneous separatrix and reach point R inside the right loop. The actual outcome depends upon its initial energy H_0 as well as upon ΔH given by eq.(13). Since the separatrix corresponds to H = 0 for all t, the post–transit value of H,

$$H_1 = H_0 + \Delta H \tag{14}$$

will determine if the motion lies inside the separatrix (if $H_1<0$) or outside the separatrix (if $H_1>0$). The theory is inapplicable to those trajectories which map to $H_1 = 0$ (i.e. which lie on the "stable manifold" of the origin) and to a small open set of trajectories around them [12].

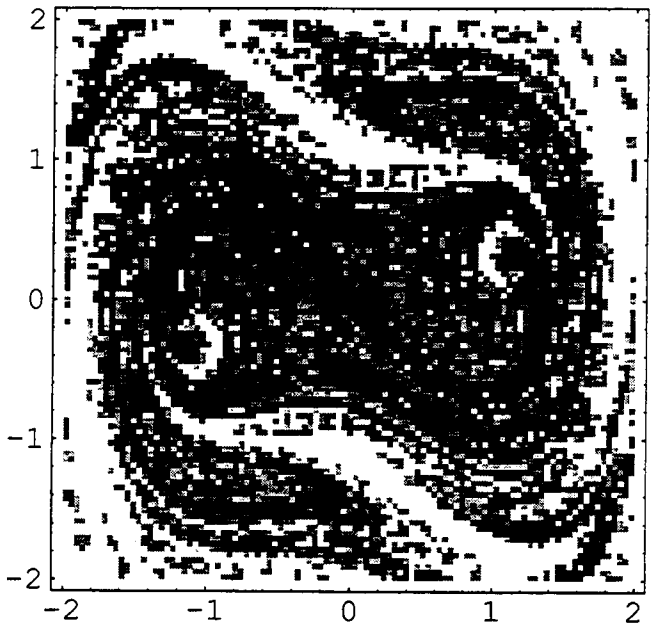

Fig.9a. RLO .02–insensitivity plot for the nonlinear Meissner eq.(2) with $\epsilon = 0.3$. A region of the x–x′ plane is displayed. Insensitivity is color–coded with six shades of grey. White corresponds to an insensitivity of 5 or greater, and black to an insensitivity of 0. Results obtained from exact elliptic function solution of eq.(2).

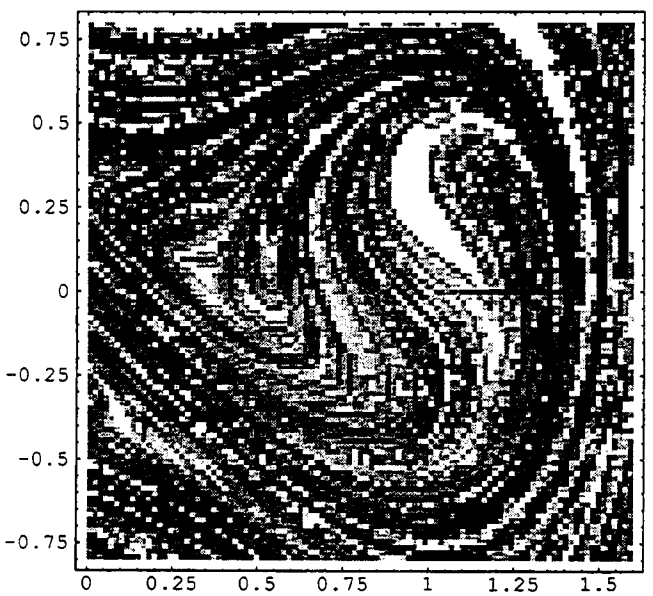

Fig.9b. RLO .0075–insensitivity plot for the nonlinear Meissner eq.(2) with $\epsilon = 0.3$. A region of the x–x′ plane is displayed. Insensitivity is color–coded with six shades of grey. White corresponds to an insensitivity of 5 or greater, and black to an insensitivity of 0. Results obtained from exact elliptic function solution of eq.(2).

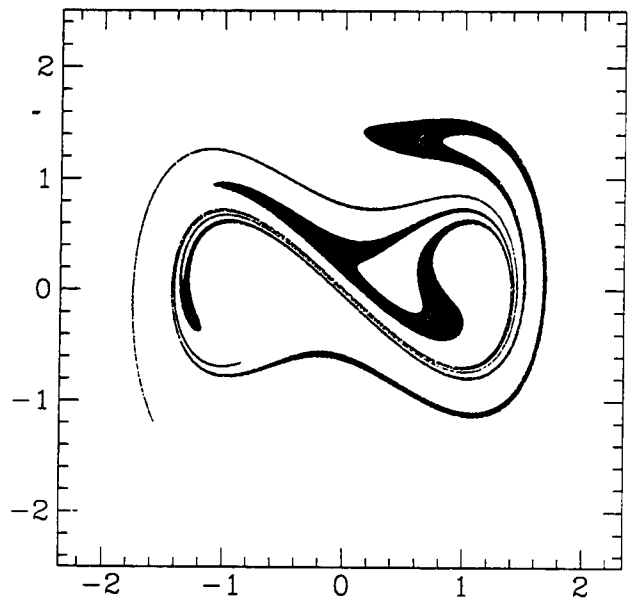

Fig.10. The set S_{-1} for the nonlinear Meissner eq.(2) with $\epsilon = 0.3$. Displayed is a map, backwards in time for one forcing period, of initial conditions in the x–x′ plane located inside the right separatrix loop . Thus S_{-1} is the boundary of the darkened region. Since only the right loop is mapped, we see only half of the set S_{-1}. The missing part is a reflection in the origin of the part shown.

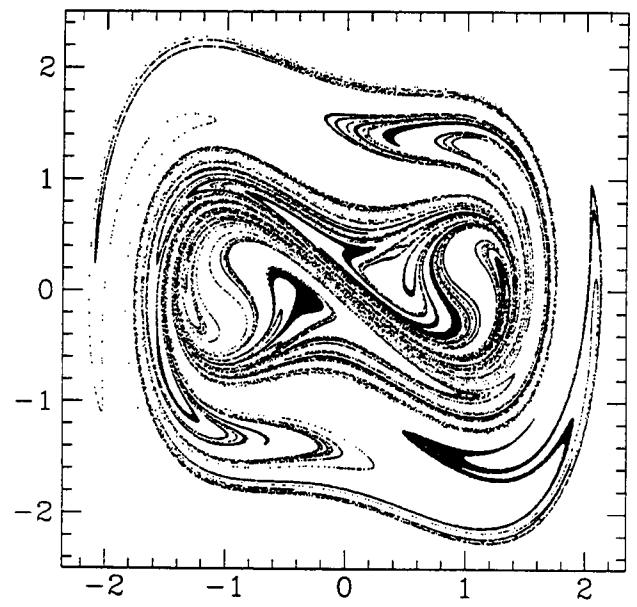

Fig.11. The set S_{-2} for the nonlinear Meissner eq.(2) with $\epsilon = 0.3$. Displayed is a map, backwards in time for two forcing periods, of initial conditions in the x–x′ plane located inside the right separatrix loop . Thus S_{-2} is the boundary of the darkened region. Since only the right loop is mapped, we see only half of the set S_{-2}. The missing part is a reflection in the origin of the part shown.

In order to estimate the time of transit Δt associated with the change in energy ΔH, Cary et al.[5] have shown that it is accurate to assume that the motion spends most of its time near the origin (where the vector field is nearly zero.) Let $T(H)$ represent the time of transit around one of the frozen loops at energy H, e.g. from U to D or from R to R. Then we can approximate the time of transit Δt when time is not frozen by the average [5]:

$$\Delta t = \tfrac{1}{2}[T(H_0) + T(H_1)] \tag{15}$$

Using the elliptic function solution to eq.(4), we find [7]:

$$T(H) = \begin{cases} \dfrac{2\ K(k)}{[4\ H + f^2\ ]^{1/4}}, & H > 0 \text{ (outside the loops)} \\ \dfrac{(2/k)\ K(1/k)}{[4\ H + f^2\ ]^{1/4}}, & H < 0 \text{ (inside a loop)} \end{cases} \tag{16}$$

where $K(k)$ is the complete elliptic integral of the first kind, and where k is its modulus,

$$k^2 = \tfrac{1}{2} + \frac{f}{2\ [4\ H + f^2]^{1/2}} \tag{17}$$

Using eqs.(13) and (15)–(17) for ΔH and Δt, we may generate a sequence of associated energies H_i, times t_i, and axis points $\sigma_i = \{U,R,D \text{ or } L\}$. For small ϵ, many such transits around the separatrix loops will occur during one forcing period. The symbol sequence in this problem which is analogous to the RLO sequence of eqs.(1) and (2) will be generated from the sequence of axis points σ_i by choosing the σ_k symbol corresponding to the time t_k closest to each of the once–per–forcing–cycle stroboscopic times $0, 1/\epsilon, 2/\epsilon, \ldots$ at which RLO sampling is to occur. For example, for the initial condition

$$H_0 = -.250,\ t_0 = 0,\ \sigma_0 = R \tag{18}$$

and ϵ=0.01, we find the results in Table 1.

Table 1

i	H_i	t_i	σ_i
0	−.250	0	R
1	−.239	4.02	R
2	−.207	8.12	R
3	−.155	12.38	R
4	−.089	16.99	R
5	−.014	22.58	R
6	.062	28.37	D
7	.128	33.29	U
8	.182	37.76	D
9	.212	42.00	U
10	.245	46.10	D
11	.252	50.14	U
12	.243	54.19	D
13	.219	58.29	U
14	.179	62.54	D
15	.124	67.03	U
16	.057	72.00	D
17	−.019	77.69	L
18	−.094	83.14	L
19	−.160	87.72	L
20	−.211	91.96	L
21	−.243	96.05	L
22	−.254	100.06	L
23	−.242	104.07	L

The RLO sequence corresponding to this initial condition would begin RL since the closest time in Table 1 to the first stroboscopic time $1/\epsilon$=100 is t_{22}=100.06 and σ_{22}=L. In this way we can generate a RLO sequence for a given initial condition (H_0,t_0).

Let us now investigate the dependence of RLO sequences in eq.(7) on initial conditions. Since the states (H_i,t_i) correspond only to points on the coordinate axes, we must revise our definition of RLO insensitivity for this case. The RLO δ–insensitivity of an initial condition P is defined as the minimum RLO propinquity for the two neighboring initial conditions which are located at a distance δ from P on the same coordinate axis. Fig.14 shows a plot of the .0005–insensitivity for eqs.(7),(8) with ϵ = .01 for a variety of initial conditions H_0, all for t_0 = 0. Note that there is a lot of nonuniformity in Fig.14. Some points have insensitivities of 1 or 2 (i.e. their RLO sequences are highly sensitive to a small change in initial conditions), while nearby points may lie in the "chimneys" of high insensitivity.

We may understand some of these features in Fig.14 by comparing it to Fig.15 which displays a first return map showing $H(t=1/\epsilon)$–H_0 versus H_0, where $H(t=1/\epsilon)$ is the energy after one forcing cycle starting from the initial condition $H(t=0)=H_0$, i.e., $H(t=1/\epsilon)$ is the energy H_k corresponding to the time t_k closest to the stroboscopic time $1/\epsilon$.

The zeros of Fig.15 represent initial conditions which approximately correspond to periodic motions. The reason for the word "approximately" in the previous sentence is that the stroboscopic time does not in general coincide with the time t_k. A zero of Fig.15 corresponds to a stable periodic motion [9] if the curve's slope lies between 0 and −2. Detailed inspection of Figs.14 and 15 reveals that most of the chimneys of insensitivity in Fig.14 overlap stable periodic motions in Fig.15. Some chimneys which do not overlap stable periodic motions in Fig.15 have been shown to correspond to stable periodic motions of the second return map, or of a higher order return map. Thus a stable periodic motion has associated with it a region of initial conditions which exhibit RLO sequences with large mutual propinquities, i.e. there is very little local chaos. This is reminiscent of the behavior observed in Poincare maps in KAM (near–integrable) situations, namely that islands of order surrounding stable periodic motions lie in the sea of chaos associated with the separatrices of unstable periodic motions.

In fact the initial conditions in Fig.14 which show the lowest RLO insensitivities correspond to the points which get mapped after one forcing period to the saddle at the origin. These points correspond to the upward peaks in Fig.15 which involve large positive changes in energy. As mentioned above, the separatrix crossing theory upon which this work is based is inapplicable to such points [12] and to a small region of initial conditions in their neighborhood. However, for small ϵ, this forbidden region has negligible measure.

The narrowness of the peaks in Fig.15 accounts for another phenomena, namely that most RLO sequences generated by this separatrix crossing model involve either all O's (those points starting with $H_0>0$, outside the separatrix loops), or no O's (those points starting with $H_0<0$, inside the separatrix loops). The latter points have RLO sequences made up of mainly R's and L's. In order for a RLO sequence to have an R followed by an O, for example, a motion would have to nearly get swallowed up by the origin, corresponding to the upward peaks in Fig.15, which involve a small set of initial conditions since they are very narrow. Motions which nearly fall into the origin may get delayed there for a long enough time that they are still outside the separatrix loops after one forcing period. This behavior is in contrast to more typical motions, that of Table 1, for example, which involve exiting out of a separatrix loop during the half of the cycle when the loops are decreasing in size, and entering into a separatrix loop in the other half of the cycle. Of course, the sequence of R's and L's may still exhibit SDIC.

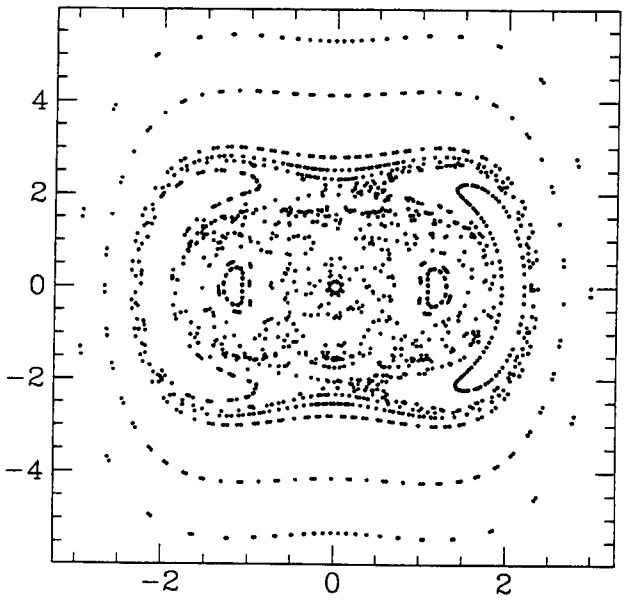

Fig.12. Poincare map of the x–x′ plane for one forcing period of the nonlinear Mathieu eq.(1) with $\epsilon = 1.6$. Note the familiar KAM pattern of islands of order in a sea of chaos [11]. The value of ϵ was chosen such that the origin is stable, based on a WKB perturbation analysis [4] of the linear Mathieu eq.(6). Map obtained by numerical integration of eq.(1).

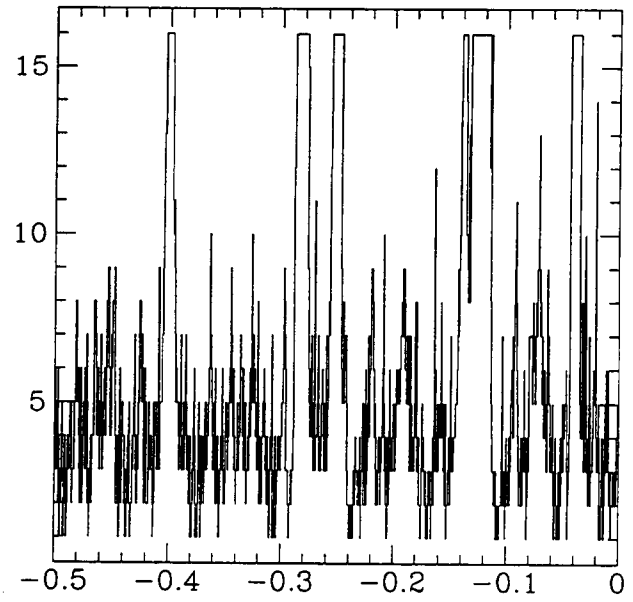

Fig.14. RLO .0005–insensitivity plot for eqs.(7),(8) with $\epsilon = .01$ from separatrix crossing theory. The horizontal axis represents initial energies H_0 for $t_0 = 0$. The vertical axis is RLO insensitivity.

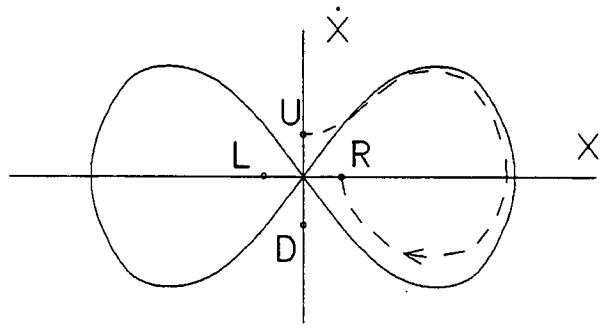

Fig.13. The points U,R,D and L represent points of intersection of a trajectory with the coordinate axes. A point starting at U may travel to R as shown, or (more typically) it may travel to D. Similarly, a point starting at R may go to either R or D; a point starting at D may go to either U or L; a point starting at L may go to either L or U. The transits which involve separatrix crossings occur less frequently than those which do not.

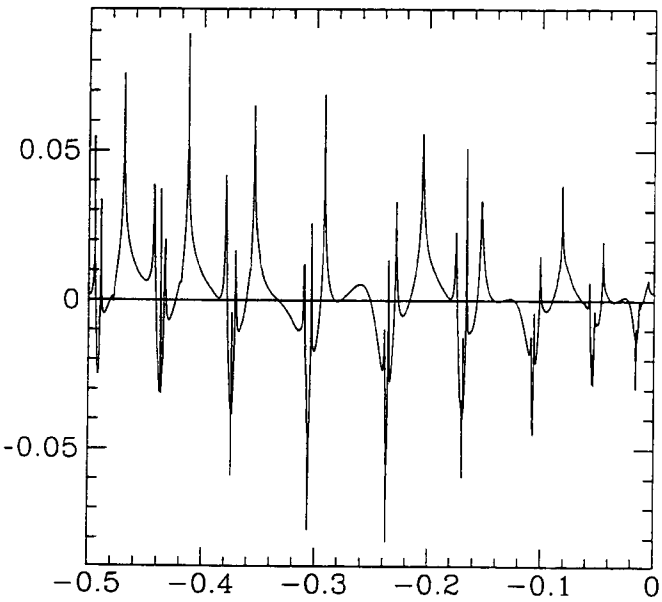

Fig.15. A first return map for eqs.(7),(8) with $\epsilon = .01$ from separatrix crossing theory. The horizontal axis represents initial energies H_0 for $t_0 = 0$. The vertical axis represents $H(t=1/\epsilon)–H_0$.

CONCLUSIONS

We have investigated the dynamics of a class of systems which possess a figure–eight separatrix which disappears periodically on a slow time scale. The behavior of such a system naturally leads to consideration of the stroboscopic location of the system in phase space, and to the RLO sequences studied in this paper. These symbol sequences have been shown to exhibit sensitive dependence on initial conditions (SDIC), a criterion often used for describing chaos.

We have identified the chaos in this class of systems as coming from several sources. By appropriately modifying the dynamical system, it is possible to investigate each separately.

In the nonlinear Mathieu and Meissner eqs.(1) and (2), SDIC of the RLO sequences can be traced to the complex shape of the preimage S_{-n} of the initial instantaneous separatrix. Inspection of S_{-n} (Figs.7,8,10,11) shows the obvious effects of stretching along the unstable manifold of the saddle.

The effect of the rotation phase, in which the origin is an instantaneous center, can be assessed by considering the linear versions of eqs.(1) and (2). We find that for those values of ϵ for which the origin is stable, the Poincare map involves a quasiperiodic rotation, a circle map. While not chaotic in itself, this behavior adds to the complexity of the dynamics.

The fact that the rotation phase is not necessary for RLO chaos can be demonstrated by modifying eq.(1) so that the origin remains saddle–like at all times. The dynamics of the modified system eq.(7) can be investigated analytically by using separatrix crossing theory, which assumes that motions remain in the vicinity of the separatrix for all time. The resulting RLO SDIC, Fig.14, shows nonuniform fine structure, similar to that which was observed in eqs.(1),(2), cf.Figs.6,9.

Although the slow evolution of the instantaneous separatrix is a source of chaos in both eq.(7) and eq.(1), it is not necessary for chaos. This follows from the chaotic behavior of eq.(2), which has no such slow evolution. Rather, the RLO chaos in the nonlinear Meissner eq.(2) can be attributed to the combined effects of quasiperiodicity a) in the rotation phase and b) inside the separatrix loops in the half of the cycle when they exist.

Finally, we note that the chaotic effects which we have just discussed occur in addition to Hamiltonian chaos, which is present here as it is in virtually all near–integrable Hamiltonian systems.

ACKNOWLEDGEMENT

The authors wish to thank Professors Philip Holmes and Timothy Healey of Cornell University for helpful discussions.

REFERENCES

1. Beigie,D., Leonard,A. and Wiggins,S.
Chaotic Transport in the Homoclinic and Heteroclinic Tangle Regions of Quasiperiodically Forced Two–Dimensional Dynamical Systems
Nonlinearity 4:775–819 (1991)

2. Bosley,D.L. and Kevorkian,J.
Sustained Resonance in Very Slowly Varying Oscillatory Hamiltonian Systems
SIAM J.Appl.Math. 51:439–471 (1991)

3. Bourland,F.J. and Haberman,R.
Separatrix Crossing: Time–Invariant Potentials with Dissipation
SIAM J.Appl.Math. 50:1716–1744 (1990)

4. Bridge,J.
Chaos and Symbol Sequences in Systems with a Periodically–Disappearing Figure–Eight Separatrix
Ph.D.thesis, Cornell University (1992)

5. Cary,J.R., Escande,D.F. and Tennyson,J.L.
Adiabatic–invariant Change due to Separatrix Crossing
Phys.Rev.A 34:4256–4275 (1986)

6. Cary,J.R. and Skodje,R.T.
Phase Change Between Separatrix Crossings
Physica D 36:287–316 (1989)

7. Coppola,V.T. and Rand,R.H.
Chaos in a System with a Periodically Disappearing Separatrix
Nonlinear Dynamics 1: 401–420 (1990)

8. Elskens,Y. and Escande,D.F.
Slowly Pulsating Separatrices Sweep Homoclinic Tangles where Islands must be Small: An Extension of Classical Adiabatic Theory
Nonlinearity 4:615–667 (1991)

9. Guckenheimer,J. and Holmes,P.
Nonlinear Oscillations, Dynamical Systems and Bifurcations of Vector Fields
Springer (1983)

10. Henrard,J.
Capture into Resonance: An Extension of the Use of Adiabatic Invariants
Celestial Mechanics 27:3–22 (1982)

11. Lichtenberg,A.J. and Lieberman,M.A.
Regular and Stochastic Motion
Springer (1983)

12. Lochak,P. and Meunier,C.
Multiphase Averaging for Classical Systems
Springer (1988)

13. Kaper,T.J. and Wiggins,S.
Lobe Area in Adiabatic Hamiltonian Systems
Physics D 51:205–212 (1991)

14. Neishtadt,A.I.
Passage Through a Separatrix in a Resonance Problem with a Slowly–Varying Parameter
J.Appl.Math.Mech. (PMM) 39:594–605 (1975)

15. Shaw,S.W. and Wiggins,S.
Chaotic Dynamics of a Whirling Pendulum
Physica D 31:190–211 (1988)

16. Stoker,J.J.
Nonlinear Vibrations
Interscience, N.Y. (1950)